

Supporting Information for

Optimization of NiMo catalytic electrode based on the distribution map of HER onset potential

Xuyang Ma,^a Jiqiang Dong,^a Fuying Li,^a Kaijie Ma,^b Le Liu^{*a} and Jingyu Xi^{*a}

Contents for supporting information

Table S1 2⁴-factor design of NiMo catalyst experiment for electrodeposition on nickel foam substrate

Table S2 16 groups of electrode samples under 2⁴-factor design

Table S3 Preparation conditions of 16 groups of electrode samples

Table S4 Width and median of box plot of 16 groups of electrode surface onset potential under 2⁴-factor design

Table S5 ANOVA table of 2⁴-factor design

Figure S1 16 groups of nickel foam substrate NiMo electrodes to be tested

Figure S2 The HER onset potential distribution maps 16 groups under 2⁴-factor design

Figure S3 LSV test plots for the investigation of optimal electrode preparation parameters

Figure S4 XRD pattern of NiMo electrode samples

Figure S5 XRS pattern of NiMo electrode samples

Figure S6 EDS pattern of NiMo electrode samples

Figure S7 Experimental results of commercial HER electrode testing

Table S1 2⁴-factor design of NiMo catalyst experiment for electrodeposition on nickel foam substrate

$c(\text{Mo}^{6+})$ (M)	$c(\text{Ni}^{2+})$ (M)	Current density (mA cm ⁻²)	Electrodeposition time (min)
0.1	0.2	20	5
0.3	0.6	60	15

Table S2 16 groups of electrode samples under 2⁴-factor design

Number	$c(\text{Mo}^{6+})$ (M)	$c(\text{Ni}^{2+})$ (M)	Current density (mA cm ⁻²)	Electrodeposition time (min)
E1	0.1	0.2	20	5
E2	0.1	0.2	20	15
E3	0.1	0.2	60	5
E4	0.1	0.2	60	15
E5	0.1	0.6	20	5
E6	0.1	0.6	20	15
E7	0.1	0.6	60	5
E8	0.1	0.6	60	15
E9	0.3	0.2	20	5
E10	0.3	0.2	20	15
E11	0.3	0.2	60	5
E12	0.3	0.2	60	15
E13	0.3	0.6	20	5
E14	0.3	0.6	20	15
E15	0.3	0.6	60	5
E16	0.3	0.6	60	15

Table S3 Preparation conditions of 16 groups of electrode samples

Number	$m(\text{Na}_2\text{MoO}_4 \cdot 2\text{H}_2\text{O})$ (g)	$m(\text{NiSO}_4 \cdot 6\text{H}_2\text{O})$ (g)	Current density (mA cm ⁻²)	Electrodeposition time (min)
E1	0.7259	1.5771	32	5
E2	0.7259	1.5771	32	15
E3	0.7259	1.5771	96	5
E4	0.7259	1.5771	96	15
E5	0.7259	4.7313	32	5
E6	0.7259	4.7313	32	15

E7	0.7259	4.7313	96	5
E8	0.7259	4.7313	96	15
E9	2.1776	1.5771	32	5
E10	2.1776	1.5771	32	15
E11	2.1776	1.5771	96	5
E12	2.1776	1.5771	96	15
E13	2.1776	4.7313	32	5
E14	2.1776	4.7313	32	15
E15	2.1776	4.7313	96	5
E16	2.1776	4.7313	96	15

Table S4 Width and median of box plot of 16 groups of electrode surface onset potential under 2⁴-factor design

Number	width	medium	Number	width	medium
E1	34.2665	-93.2968	E9	35.4749	-107.6578
E2	19.3539	-94.9986	E10	22.4768	-98.1943
E3	19.2211	-90.1356	E11	28.9047	-71.3266
E4	26.4451	-111.7350	E12	28.4327	-80.3224
E5	54.8589	-229.3337	E13	22.0687	-227.6721
E6	55.0508	-179.5065	E14	46.1354	-187.0731
E7	48.7247	-100.5535	E15	73.0257	-116.5413
E8	39.3342	-74.0863	E16	34.3213	-64.6350

Table S5 ANOVA table of 2⁴-factor design

Source	Sum of Squares	df	Mean Square	F Value	p-value Prob>F	
A-Mo ⁶⁺	1078.67	1	1078.67	0.83	0.3822	not significant
B-Ni ²⁺	6423.45	1	6423.45	4.93	0.0483	significant
C-Current density	9862.89	1	9862.89	7.58	0.0188	significant
D-Electrodeposition time	75.77	1	75.77	0.058	0.8138	not significant

Figure S1 16 groups of nickel foam substrate NiMo electrodes to be tested

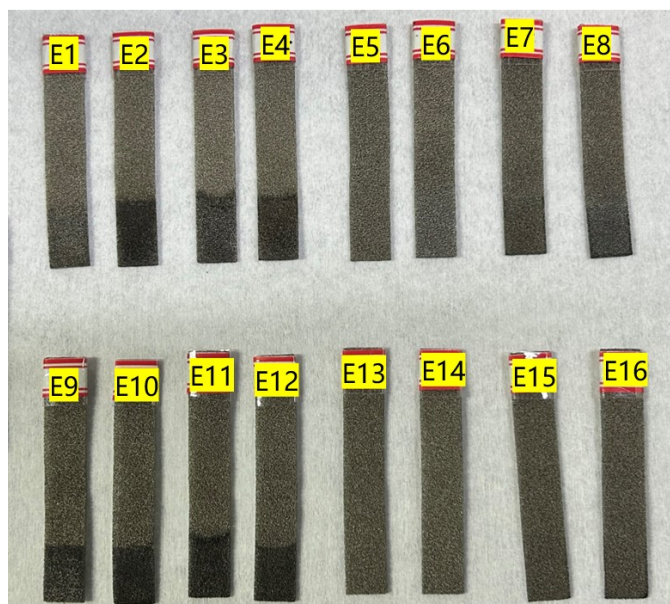


Figure S1 shows 16 sets of electrodes E1-E16 prepared by the electrodeposition method, the average immersion depth is 1.6 cm and the area of the deposited catalytic electrodes is 1.6 cm^2 . The electrodes are removed and rinsed with deionized water and anhydrous ethanol and dried naturally after deposition.

Figure S2 The HER onset potential distribution maps 16 groups under 2^4 -factor design

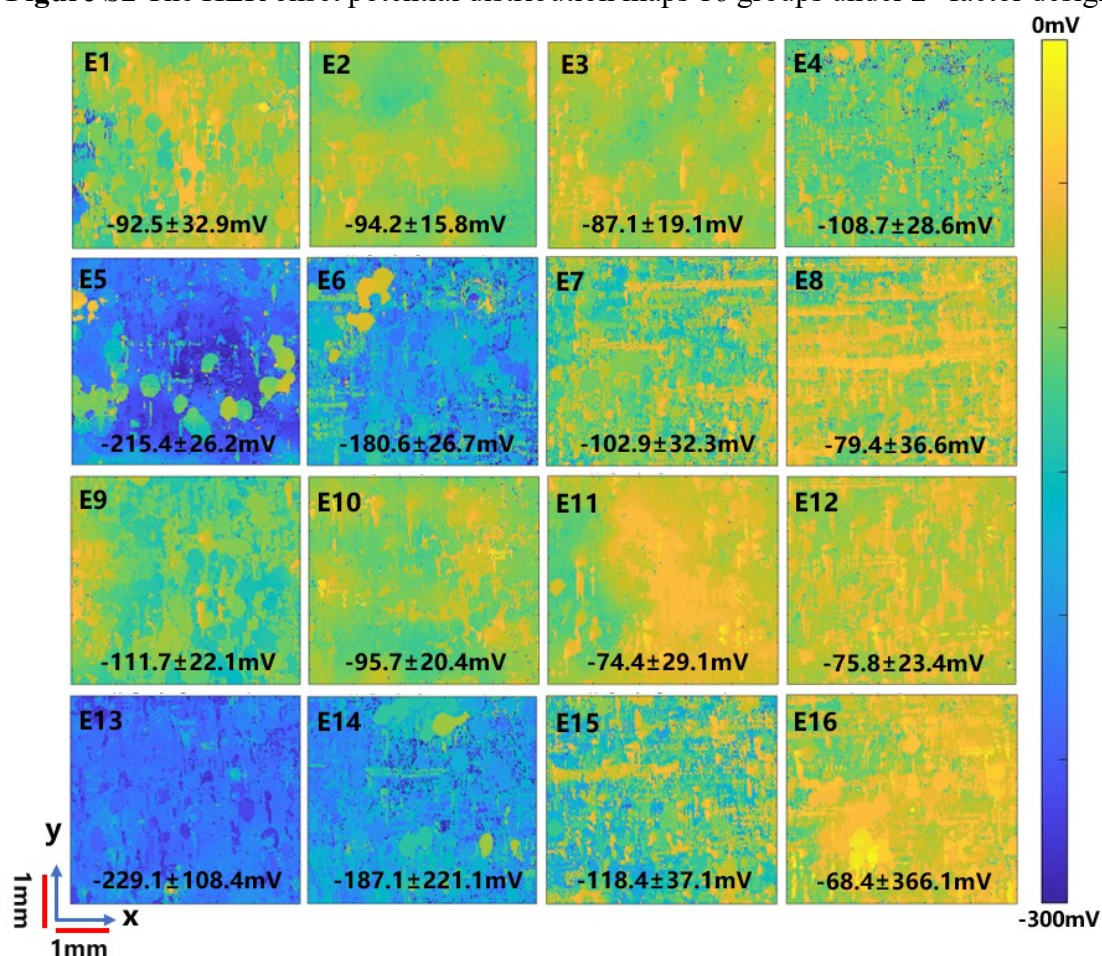


Figure S2 shows the initial potential distribution of 16 groups of electrodes after the test and the "mean \pm standard deviation" is labelled. It can be seen that the uniformity of electrode E2 is better and the overall catalytic activity of electrode E16 is better, but its uniformity is poor. On the other hand, the distribution plots of electrodes E5, E6, E13 and E14 are blue, indicating that their catalytic activity is poor.

Figure S3 LSV test curves for the investigation of optimal electrode preparation parameters

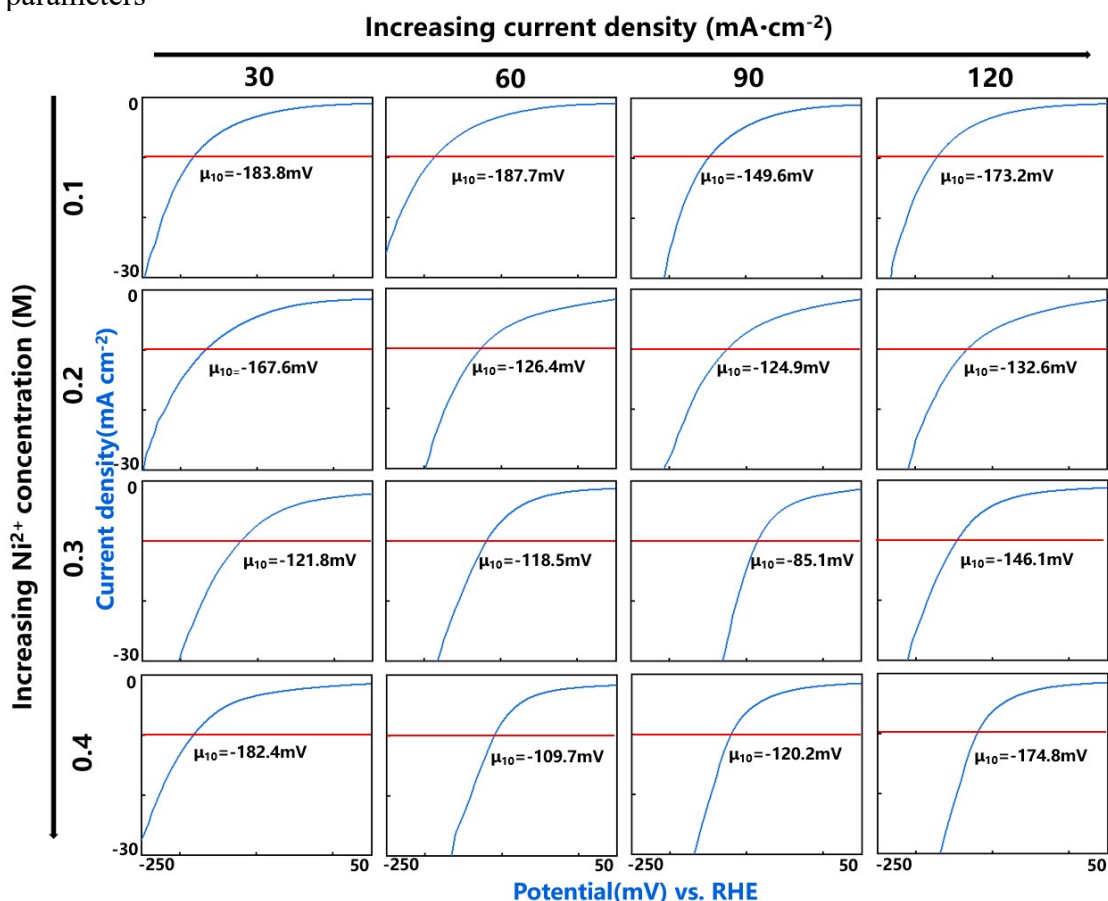


Figure S3 displays the LSV test curves for 16 groups of electrodes when exploring optimal electrode preparation conditions. The figure indicates a minimum overpotential at a Ni^{2+} concentration of 0.3 M and a current density of 90 mA cm^{-2} , which is consistent with the distribution map of HER onset potential.

Figure S4 XRD pattern of NiMo electrode samples

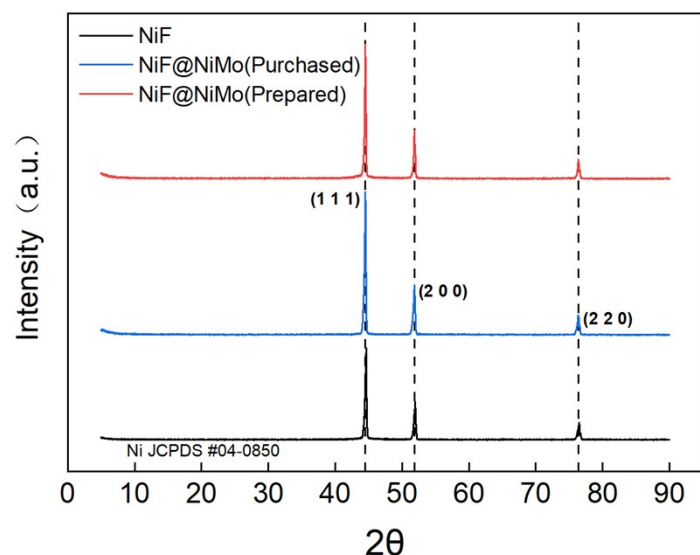


Figure S4 represents the XRD patterns recorded for NiMo electrode samples with different Mo content. The figure displays the XRD curves of pure nickel foam (black line), a purchased commercial NiMo electrode (blue line), and an experimentally prepared NiMo electrode (red line). The diffraction peaks located at $2\theta \approx 44.6^\circ$, 51.8° , and 76.4° are assigned to the (111), (200), and (220) Ni facets, respectively (JCPDS No. 04-0850). The absence of distinct Mo peaks indicates that the plated layer has no single phase of Mo. Noticeably, there is no obvious peak for NiMo alloy due to the small actual Mo concentration. However, diffraction peaks shifted toward the lower 2θ values, which can be attributed to the lattice expansion due to the successful incorporation of Mo into Ni¹.

Figure S5 XPS pattern of NiMo electrode samples

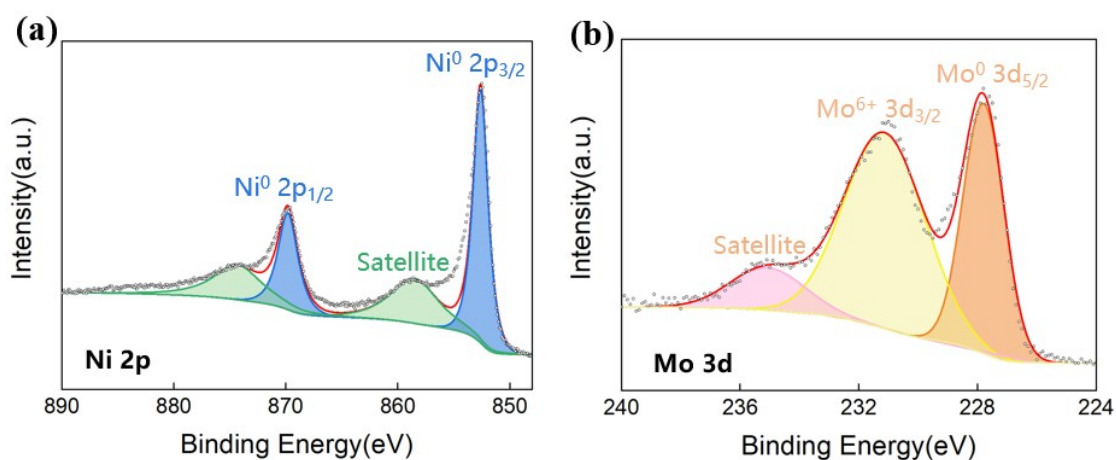


Figure S5 represents the EDS patterns recorded for the NiMo electrode prepared by the experiment. To further confirm the chemical composition and electronic states of the

prepared nanowire arrays electrode, an X-ray photoelectron spectroscopy (XPS) investigation was conducted. Figure S5a-b represents the XPS spectra of the NiMo electrode for Ni 2p and Mo 3d, respectively. Ni 2p spectrum shows two main peaks at 852.6 and 869.5 eV, accompanied by two broad satellite peaks, which correspond to metallic Ni.² While, in the case of the Mo 3d spectrum, the prominent peak appearing at 227.9 eV can be indexed to metallic Mo, and the peak located at 231.1 eV is referred to as the Mo⁶⁺ state.³

Figure S6 EDS pattern of NiMo electrode samples

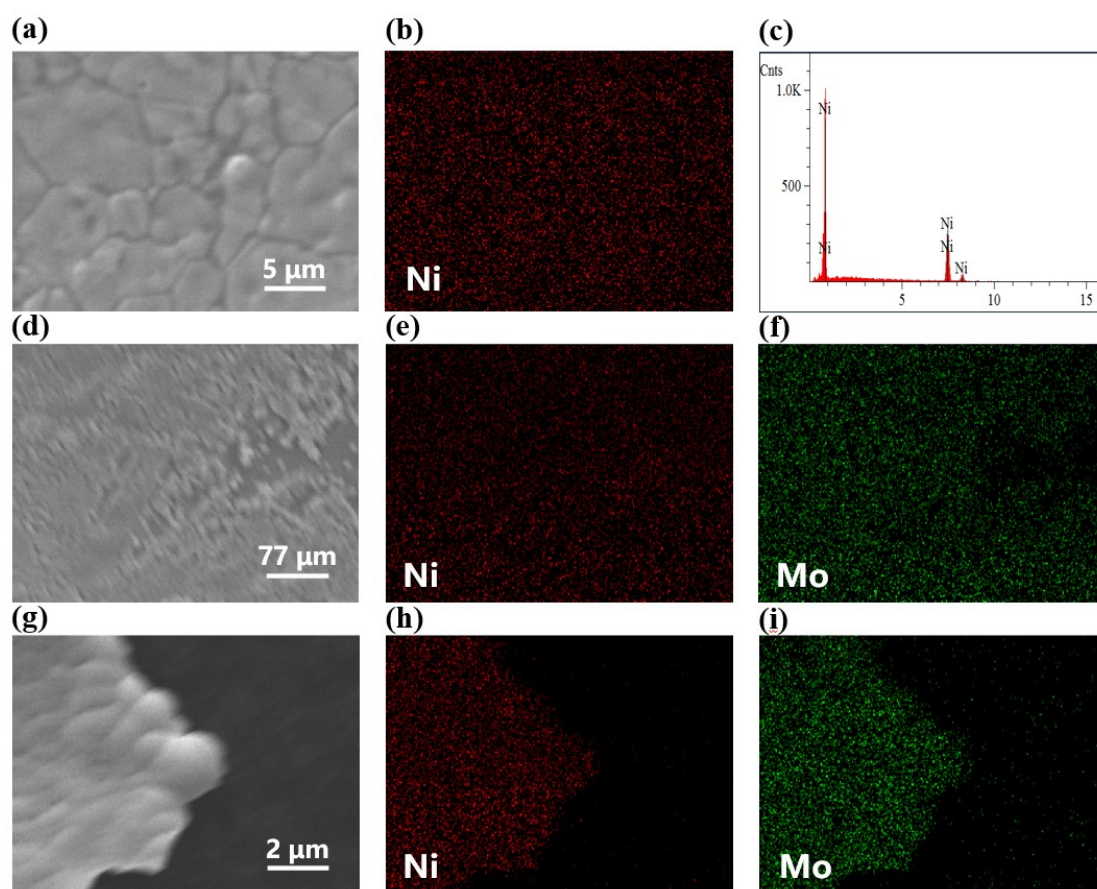
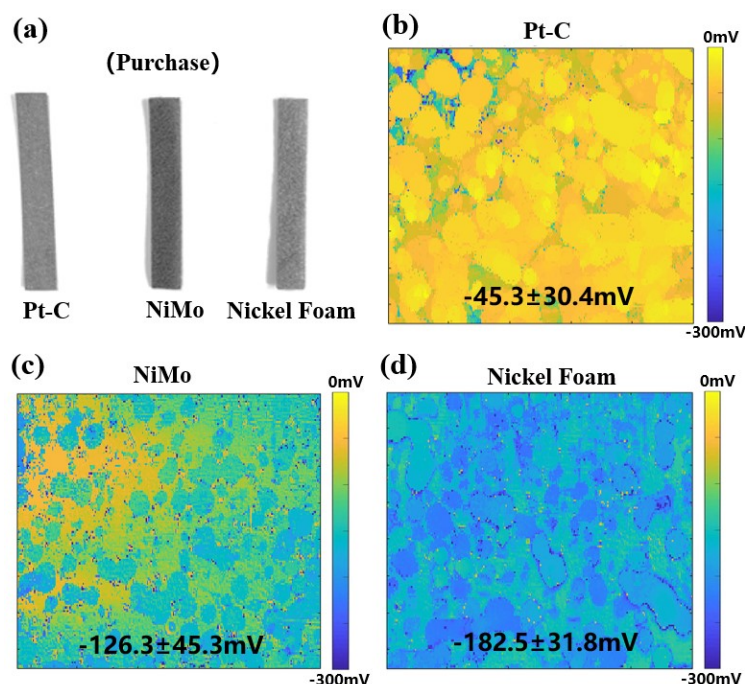


Figure S6 represents the EDS patterns recorded for NiMo electrode samples with different Mo content. Figures S6a-c show SEM maps and Ni and Mo elemental mapping images of pure nickel foam, Figures S6d-f show corresponding figures of purchased commercial NiMo electrodes, and Figures S6g-i show corresponding figures of NiMo electrodes prepared by experiment. The figure illustrates that the commercial NiMo electrodes purchased have slightly uneven Ni and Mo elements. Figures S6g-i demonstrate that NiMo coatings were successfully obtained through electrodeposition experiments with good uniformity.

Figure S7 Experimental results of commercial HER electrode testing



Commercial HER catalytic electrodes, including platinum-plated carbon felts (Pt-C) and nickel-molybdenum foam (NiMo) electrodes, were purchased. A nickel foam (NiF) material without any catalyst loading was used as a control. The electrodes underwent cleaning before examination with the TIRi detection device. The resulting data was processed to produce onset potential distribution maps. The colorbar of the distribution maps was chosen to match the content of the main text, and the values marked on the plots were labeled as 'mean \pm standard deviation'.

Figures S7b-d demonstrate the onset potential distribution of Pt-C, NiMo, and NiF. The catalytic performance of the Pt-C catalytic electrode is best observed through its color, with an average value of only -45.3 mV, indicating superior performance. The catalytic performance of the purchased NiMo electrode was superior to that of pure nickel foam. This is supported by the lower average index value compared to nickel foam. However, the homogeneity of the NiMo electrode was poorer, with a value of 45.3 mV, which was the highest among the three electrodes tested. This suggests that industrially produced and commercially available HER catalytic electrodes may have good overall performance but uneven distribution. The NiMo electrodes prepared under the optimal conditions in this research exhibit superior overall performance and homogeneity (mean value: -51.6 mV, standard deviation value: 15.3 mV) compared to the purchased NiMo electrodes, demonstrating the significance of this research.

Reference

1. D. Gao, J. N. Guo, X. Cui, L. Yang, Y. Yang, H. C. He, P. Xiao and Y. H. Zhang, *ACS Appl. Mater. Interfaces*, 2017, **9**, 22420-22431.
2. X. D. Yan, L. H. Tian and X. B. Chen, *J. Power Sources*, 2015, **300**, 336-343.
3. X. Q. Wang, R. Su, H. Aslan, J. Kibsgaard, S. Wendt, L. H. Meng, M. D. Dong, Y. D. Huang and F. Besenbacher, *Nano Energy*, 2015, **12**, 9-18.